JACS
JOURNAL OF THE AMERICAN CHEMICAL SOCIETY
Article
pubs.acs.org/JACS

Mechanism of Acyl–Enzyme Complex Formation from the Henry–Michaelis Complex of Class C β-Lactamases with β-Lactam Antibiotics

Ravi Tripathi and Nisanth N. Nair*

Department of Chemistry, Indian Institute of Technology Kanpur, 208016 Kanpur, India

Supporting Information

ABSTRACT: Bacteria that cause most of the hospital-acquired infections make use of class C β-lactamase (CBL) among other enzymes to resist a wide spectrum of modern antibiotics and pose a major public health concern. Other than the general features, details of the defensive mechanism by CBL, leading to the hydrolysis of drug molecules, remain a matter of debate, in particular the identification of the general base and role of the active site residues and substrate. In an attempt to unravel the detailed molecular mechanism, we carried out extensive hybrid quantum mechanical/molecular mechanical Car–Parrinello molecular dynamics simulation of the reaction with the aid of the metadynamics technique. On this basis, we report here the mechanism of the formation of the acyl–enzyme complex from the Henry–Michaelis complex formed by β-lactam antibiotics and CBL. We considered two β-lactam antibiotics, namely, cephalothin and aztreonam, belonging to two different subfamilies. A general mechanism for the formation of a β-lactam antibiotic–CBL acyl–enzyme complex is elicited, and the individual roles of the active site residues and substrate are probed. The general base in the acylation step has been identified as Lys_{67}, while Tyr_{150} aids the protonation of the β-lactam nitrogen through either the substrate carboxylate group or a water molecule.

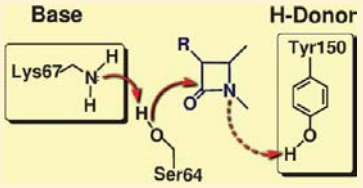

1. INTRODUCTION

β-Lactam antibiotics target the bacterial cell wall biosynthetic enzymes called penicillin binding proteins (PBPs) and make them chemically inert, resulting in bacterial death. Evolutionary pressure has resulted in the expression of β-lactamases by bacteria to resist the actions of β-lactam antibiotics by breaking the amide bond of the β-lactam ring of these antibiotics through a general-base hydrolysis reaction.[1] β-Lactamases bind to β-lactam antibiotics in a fashion similar to the way the antibiotics bind to PBPs but hydrolyze them rapidly.[2,3] The bacterial resistive mechanism has evolved with great sophistication by their evolution and even shows resistance toward new-generation antibiotics, posing a great threat to public health.[4,5]

Among the four classes of β-lactamases,[6] we are concerned with the class C β-lactamases (CBLs) in this work. These enzymes are found in most of the Gram-negative bacteria[7,8] and are clinically important as they have been traced in the pathogenic organisms responsible for hospital-acquired infections.[9,10] The mechanism of hydrolysis of a β-lactam drug by these enzymes involves two steps: (a) acylation, where the Ser_{64} residue covalently binds to the β-lactam C, resulting in β-lactam ring-opening; (b) deacylation, in which the β-lactam C–$Ser_{64}O_\gamma$ bond is hydrolyzed; see Figure 1.[2,11] The acylation and the deacylation steps are irreversible, and k_2 is considered to be higher than k_3:[12]

$$E + S \underset{k_{-1}}{\overset{k_1}{\rightleftharpoons}} ES \xrightarrow{k_2} ES^* \xrightarrow{k_3} E + P$$

It is generally believed that a general-base mechanism is active in the formation of the acyl–enzyme complex (ES*) and in the following deacylation step. Discerning the details of the mechanism is valuable for the design of novel antibiotics and inhibitors.[13] In this spirit, much research has been devoted to unraveling the mechanism, in particular to scrutinizing the role of the active site residues.[4,14−18]

The active site residues that play an important role in the reaction are Lys_{67}, Lys_{315}, Ser_{64}, and Tyr_{150}.[12,19−23] X-ray studies have proven that Ser_{64} directly participates in the acylation of the β-lactam ring.[24,25] However, the roles of the other residues and the details of the proton transfer mechanism part of the acylation and deacylation are still a matter of debate.[5,14]

To understand the mechanism, it is vital to know the protonation states of the active site residues Lys_{67}, Lys_{315}, and Tyr_{150}. There are mainly four possible protonation states of the active site in class C β-lactamase,[26] among which the one where all the residues are in their protonated form and also the one where Lys_{315} is in its neutral state with the other two residues being in their protonated form have been discarded by previous studies.[26−28] The other two protonation states, where (a) Lys_{67} is protonated, Tyr_{150} is anionic, and Lys_{315} is protonated ($\mathbf{K^+Y^-}$) and (b) Lys_{67} is neutral, Tyr_{150} is protonated, and Lys_{315} is protonated (**KY**), are shown to be separated by free energy barriers of only 1 kcal mol^{-1} when cephalothin is noncovalently bound to the enzyme;[28] see Figure 2 for the nomenclature used for various protonation states. This implies that these protonation states are equally accessible at ambient conditions. Calculations of aztreonam-bound CBL indicated the preference of **KY** over the others.[26]

Various mutational, enzyme kinetics, crystallographic, and computational studies concluded that either Lys_{67} or Tyr_{150} acts

Received: May 27, 2013
Published: September 6, 2013

dx.doi.org/10.1021/ja405319n | J. Am. Chem. Soc. 2013, 135, 14679−14690

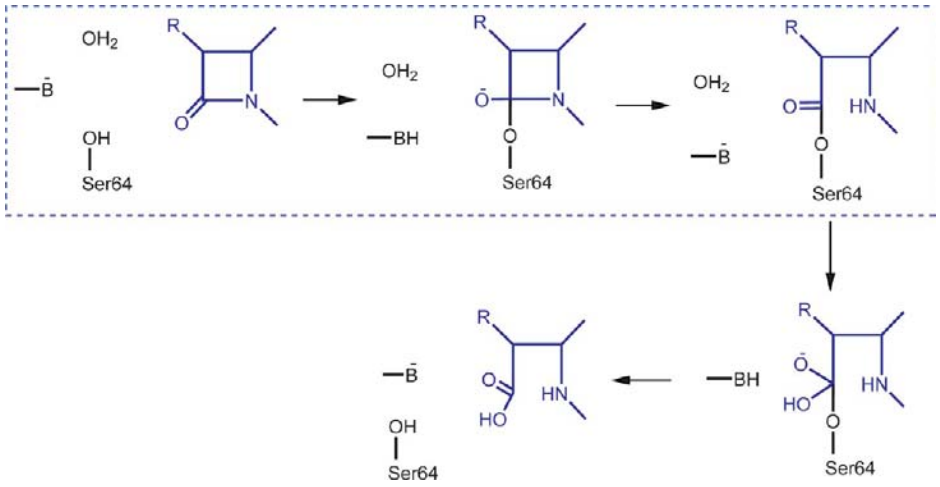

Figure 1. General mechanism of the acylation (within the dotted box) and deacylation reactions of a β-lactam antibiotic with CBL.

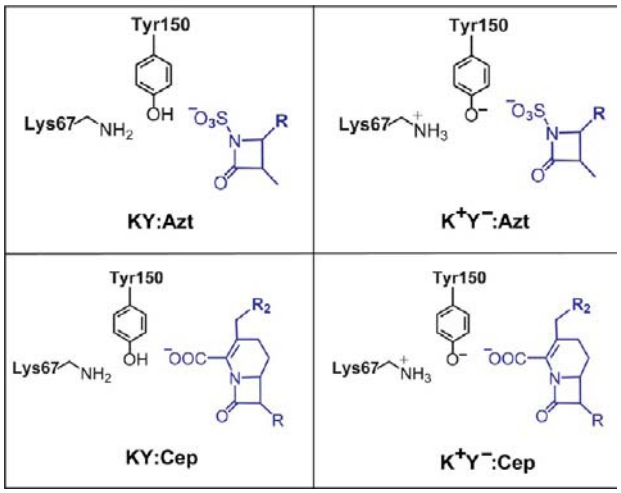

Figure 2. Various protonation states of Lys_{67} and Tyr_{150} considered in this study in the presence of aztreonam (first row) and cephalothin (second row) drug molecules. See also Supporting Information section 2.

as a base in CBL,[12,19,23,29,30] although conclusive evidence on the protonation states of these residues has not been obtained. An anionic form of Tyr_{150} was proposed and conjectured as the general base in the acylation reaction by Winkler and co-workers[24] in their pioneering work, where they crystallized CBL complexed with aztreonam at 2.5 Å resolution. Their interpretation was supported by electrostatic Poisson–Boltzmann calculations based on the low pK_a value estimated for the Tyr_{150} group (4.0–8.3) in the apoprotein.[31] Site-directed mutagenesis experiments and kinetics studies also noted the crucial role of Tyr_{150} in enzymatic activities and proposed a mechanism with Tyr_{150} as the general base.[23] Knox and co-workers, on observing a close association of $Tyr_{150}O_\eta$ with $Ser_{64}O_\gamma$ in a transition-state analogue of the tetrahedral intermediate using a phosphonate derivative of a cephalosporinase, hypothesized Tyr_{150} as a general base during the acylation reaction.[32] The same interpretation was also made for the transition-state analogue of CBL structures with a boronic acid derivative.[17,33] In addition to these, a few other studies[29,34] also supported the same hypothesis and suggested Tyr_{150} in the anionic form activates Ser_{64} for the acylation reaction. On the contrary, the possibility of Lys_{67} acting as a base was first proposed by Page and co-workers,[22] according to which Tyr_{150} does not play any direct role in acylation, especially for slowly hydrolyzing substrates, whereas Lys_{67} in its neutral form activates Ser_{64} by abstracting the proton of the latter. The ^{13}C NMR-based titration experiments observed no change in chemical shift in the pH range of 6–12, suggesting the existence of the neutral form of Tyr_{150} in the apoproteins.[35] Chen et al.[30] observed a large change in k_{cat} (61-fold) and k_{cat}/K_m (2200-fold) for the cephalothin drug with a K67R mutation of CBL, and these results together with crystallographic data led these authors to propose a cooperative role of neutral Tyr_{150} and neutral Lys_{67} in the activation of Ser_{64} and water during acylation and deacylation, respectively. A precomplexed structure with the cephalothin drug captured crystallographically shows the interaction between Tyr_{150} and the carboxylate group of cephalothin and hence indicates Tyr_{150} in its neutral state.[25] A high-resolution crystal structure of the transition-state analogue of the deacylation reaction supports the existence of neutral Tyr_{150} during the whole deacylation reaction.[36] Other than these, a third possibility has also been proposed where the carboxylate group (connected to the ring adjacent to the β-lactam ring) of the β-lactam antibiotics plays an important role during acylation reaction, thus indicating a substrate-facilitated mechanism.[25,37]

Several computational studies on the topic are also available in the literature, most of which have focused on the mechanistic aspects of the deacylation reaction. Quantum mechanical/molecular mechanical (QM/MM) calculations by Gherman et al.[27] showed that **KY** is 1.8 kcal mol^{-1} higher in energy compared to $\mathbf{K^+Y^-}$ in the cephalothin–CBL acyl–enzyme complex. Their calculations also explained why deacylation proceeds faster in CBL compared to PBPs. Interestingly, they found that the hydrogen-bonding interactions between the anionic Tyr_{150} and both protonated Lys_{67} and Lys_{315} residues are important for the activity of CBL. Hata et al.[38] also obtained a similar difference in potential energy between these two protonation states in the acyl–enzyme complex and hence considered Tyr_{150} in the deprotonated state as the base for deacylation. They have estimated the potential energy change along the deacylation reaction, where they simulated the activation of hydrolytic water by anionic Tyr_{150} followed by proton transfer from Lys_{67} to Ser_{64}. A molecular dynamics (MD) study by Díaz et al.[26] indicated that, for the aztreonam–CBL noncovalent complex, **KY** is ~20 kcal mol^{-1} more stable

dx.doi.org/10.1021/ja405319n | J. Am. Chem. Soc. 2013, 135, 14679–14690

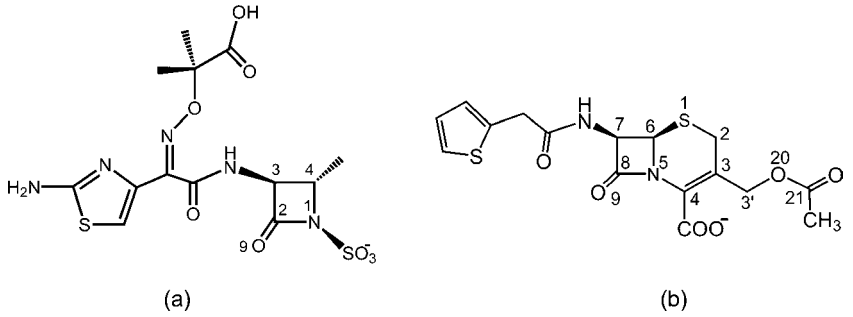

Figure 3. Structures of aztreonam and cephalothin drug molecules.

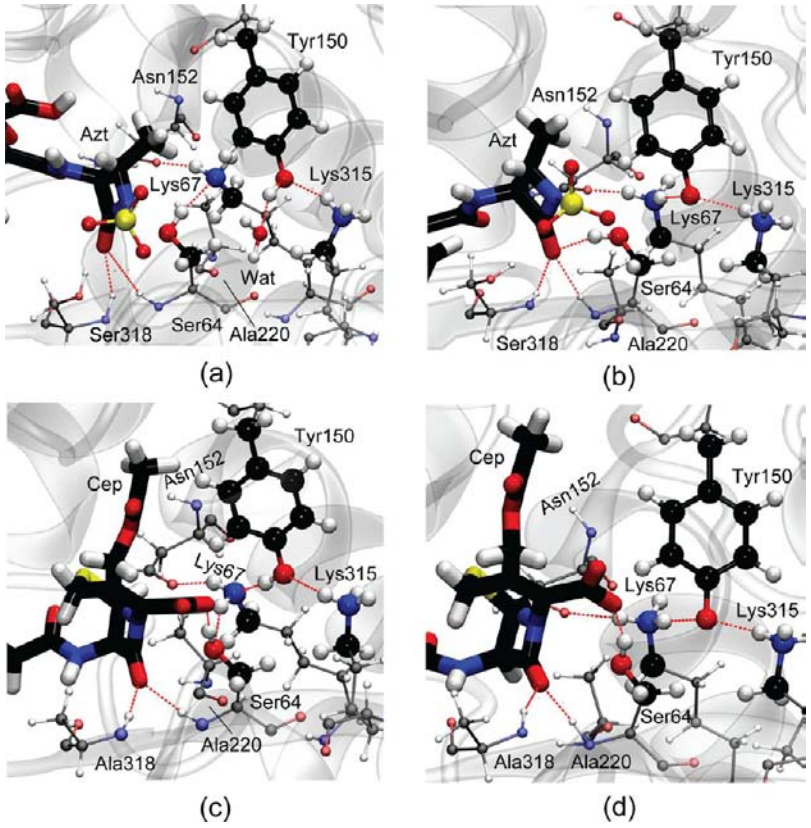

Figure 4. Equilibrated active site structure of the aztreonam−CBL complex in the (a) KY:AztB and (b) $\mathbf{K^+Y^-}$**:Azt** protonation states and the cephalothin−CBL complex in the (c) **KY:Cep** and (d) $\mathbf{K^+Y^-}$**:Cep** protonation states. For clarity the drug molecules are rendered in licorice style. Atom color codes: S (yellow); C (black); O (red); N (blue); H (white).

than $\mathbf{K^+Y^-}$. They found stable interactions between Lys_{67} and Ser_{64}, leading them to conclude Lys_{67} as the general base for the acylation reaction. On the contrary, using a QM/MM-based MD study, we reported that these two protonation states are accessible at ambient conditions in the cephalothin−CBL noncovalent complex.[28] Interestingly, in the case of the apoenzyme, these two protonation states have different free energies, with deprotonated Tyr_{150} being more stable. Sharma and Bandyopadhyay[37] looked at proton transfer of Ser_{64} to the carboxylate group of the substrate using classical force-field-based MD (of the fully solvated protein) and gas-phase QM (with the truncated model) calculations. On the basis of the pK_a calculations, they employed an active site model where Tyr_{150} and Lys_{67} were taken in their protonated forms and thus suggested a substrate-assisted pathway.

In the present study, we investigate in detail the formation of the acyl−enzyme complex by two different β-lactam antibiotic drug molecules with CBL. The two drug molecules considered belong to two different subfamilies of β-lactam antibiotics: (a) cephalothin, which is a member of the first-generation cephalosporins and is known to be hydrolyzed by CBL very efficiently;[39] (b) aztreonam, which belongs to the monobactam subfamily and is known to show better resistance (due to slow deacylation) toward hydrolysis than cephalothin[39] (see Figure 3). Although the rates of hydrolysis (k_{cat}) of these drugs are known, accurate measurements of the rates of acylation (k_2) are not available, other than estimates of their lower limits.[12]

To summarize, the outstanding questions on the mechanism of acylation are the following:

- What is the general base involved in the acylation step? As discussed above, this could be (a) Lys_{67}, (b) Tyr_{150}, or (c) the drug molecule itself.

dx.doi.org/10.1021/ja405319n | J. Am. Chem. Soc. 2013, 135, 14679−14690

- What is the mechanism of protonation of the β-lactam N? The possibilities are through (a) Lys_{67}, (b) Tyr_{150}, (c) the drug, or (d) water.
- What are the crucial drug−enzyme interactions and the role of the functional groups of the substrate?

Answering the above questions is vital in the fundamental understanding of the molecular mechanism behind the antibiotic resistance. Insights into the mechanism would help in the design of novel antibiotics and inhibitors. Certainly, the reactions involved here are very complex as they are influenced by the structure and dynamics of various side chains, the protein backbone, and the solvent.[40] Several degrees of freedom contribute directly and indirectly to the chemical reaction undergone at the active site.

As mentioned earlier, due to the relatively fast acylation step, the detailed mechanism of this process is difficult to study directly through experiments, while molecular simulation is an ideal tool to address such problems.[41] However, no study has been performed yet to understand the full acylation reaction, and only a very few static QM and QM/MM studies addressed the Ser_{64} activation[37] and deacylation[27,38] reactions by CBL. In this paper, through computationally intensive QM/MM[42] MD simulations combined with rare-event sampling,[43,44] we scrutinize the detailed mechanism of acylation of two subclasses of β-lactam antibiotics and address the aforementioned open questions related to the problem.

2. METHODS AND MODELS

2.1. System Setup and Molecular Mechanics Simulation. The starting structure of the noncovalent complex of CBL and aztreonam was constructed from the *Citrobacter freundii* class C enzymes complexed with a reacted aztreonam molecule (PDB ID 1FR6);[24] more details can be found in the Supporting Information. Two initial structures were constructed with differing protonation states of Tyr_{150} and Lys_{67} (**K^+Y^-:Azt** and **KY:Azt**) and solvated with 14 750 TIP3P water molecules in a periodic simulation box of dimensions 83 × 81 × 90 Å^3; see Figure 4. Five Na^+ and six Cl^- ions were also added to neutralize the whole system. The parm99 version of the AMBER force field[45] was used for the protein simulation, while the GAFF force field[46] was employed for describing the aztreonam molecule. Restrained electrostatic potential (RESP) derived point charges computed using RED software[47] were assigned for aztreonam. In the case of the **K^+Y^-:Azt** protonation state, RESP charges of the anionic Tyr residue were also computed using the RED software using the NME-Tyr-Ace peptide model.

Similar modeling and simulation strategies were also used in modeling the cephalothin−enzyme complex. Here the crystal structure of the wild-type AmpC β-lactamase complexed with a cephalothin drug molecule (PDB ID 1KVL)[25] was used as the starting point. Gly_{64} mutated in place of Ser_{64} in the crystal structure has been replaced back to Ser_{64}. Two protonation states, **K^+Y^-:Cep** and **KY:Cep**, were modeled in the same fashion as the aztreonam−enzyme complex discussed above; see also Figure 2 and ref 28. The box size used for the NVT MD simulation was 79 × 77 × 76 Å^3, which contained 13 599 TIP3P water molecules.

For the MM calculations, a nonbonded interaction cutoff of 15.0 Å was used. Equilibration MD simulation using the MM force field was carried out with a time step of 1 fs. After a few steps of initial energy minimization, 1 ns of NPT MD simulation was performed for both the protonation states using a Langevin thermostat at 300 K and Berendsen barostat at 1 atm. Subsequently, a 5 ns NVT MD simulation was carried out with a previously equilibrated cell volume.

2.2. QM/MM Simulation. Hybrid QM/MM[42] calculations with the substrates aztreonam and cephalothin were performed using the CPMD/GROMOS interface[48,49] with the final (equilibrated) structures obtained from the corresponding classical force field simulations, unless mentioned otherwise. In these simulations, the side chain of Ser_{64}, Lys_{67}, Tyr_{150}, Lys_{315}, the drug, and up to four water molecules within the active site were treated quantum mechanically. In the case of cephalothin, the thiophene ring was treated using MM as in ref 28. Whenever a bond was cleaved between a QM and an MM atom, capping H atoms were used for saturating bonds within the QM part. Within the protein, capping hydrogen atoms were introduced between the Cα and Cβ atoms for Tyr_{150} and Ser_{64} and between Cδ and Cε for Lys_{67} and Lys_{315}. The capping hydrogen atoms were constrained to lie along the Cα−Cβ/Cδ−Cε bond during the QM/MM MD simulations.

The sizes of the QM box were 21 × 25 × 23 and 18 × 21 × 22 Å^3 for the simulations with aztreonam and cephalothin substrates, respectively. The plane-wave density functional theory with the PBE functional[50] and ultrasoft pseudopotentials[51] were used to treat the QM part of the system. A plane-wave cutoff of 25 Ry was used here.

The QM/MM coupling was based on the electronic coupling scheme proposed by Laio et al.[48] An MM atom within 15 Å of the QM density was allowed to interact through charge density−point charge interaction, while the rest of the MM atoms interacted with multipole expansion (until the quadrapole) of the charge density interaction potential. Any MM atoms that were part of the QM/MM interaction exclusion list interacted with the remaining QM atoms through D-RESP charges of the QM atoms, as computed according to ref 52. Independent Nosé−Hoover chain thermostats[53] were employed for the QM part, the remaining protein, and the solvent. The dynamics of the QM part was determined using the Car−Parrinello MD method,[54] with a fictitious mass of 700 amu. The electronic wave function was also thermostated using the Nosé−Hoover chains. The MD time step for the QM/MM simulation was 0.125 fs.

2.3. Metadynamics. We have employed the extended Lagrangian metadynamics technique[44,55] to simulate the acylation reaction. In practice, the method relies on dynamically modifying the potential through augmenting repulsive potentials along the selected set of coordinates relevant for the chemical reaction of interest. These coordinates will be called collective coordinates, CCs, hereafter. Most crucially, since the augmented biasing potentials compensate for the free energy, the negative sum of the biasing potentials gives a map of the free energy surface (within the selected coordinates). This allows one to find the reaction coordinates (in terms of CCs), minimum energy pathways (thus the mechanism), and (Helmholtz) free energy barriers for chemical reactions. The free energy estimates here include entropic contributions (beyond the harmonic approximation) and account for finite temperature and finite solvent effects.

In the current work, we have used the extended Lagrangian metadynamics approach.[44] Here, the total dimension of the system is extended by adding additional degrees of freedom (called collective variables, CVs), each of them coupled harmonically to one of the CCs, and the biasing potentials are added directly in the CV space. The harmonic coupling constants were taken as 2.0 au for coordination number type CCs and 0.5 au for distance difference or distance type CCs. Definition of the coordination number is given in Supporting Information section 3. In all our calculations, biasing potentials were Gaussian functions with their height varied between 1 and 3 k_BT and width fixed at 0.05 unit of CCs. An adaptive metadynamics time step was used on the basis of the criterion that CVs are displaced at least 3/2 times the width of a Gaussian before addition of a new Gaussian to avoid "hill-surfing" problems.[56] The total length of the metadynamics simulations varied from 7 to 82 ps.

2.4. Accuracy. A proper selection of essential coordinates is key to the successful application of the metadynamics method. This is even more crucial for modeling reactions involving a protein, where a large number of coordinates may be directly and indirectly involved in the progress of the reaction. Since, practically, sampling more than three or four CCs is a computationally difficult task in metadynamics for such problems, not all the essential coordinates can be included in the CCs. This problem can be addressed by combining metadynamics with parallel tempering[57] or by a more eloquent bias exchange approach.[58] However, for the current problem these techniques are computationally unaffordable to us.

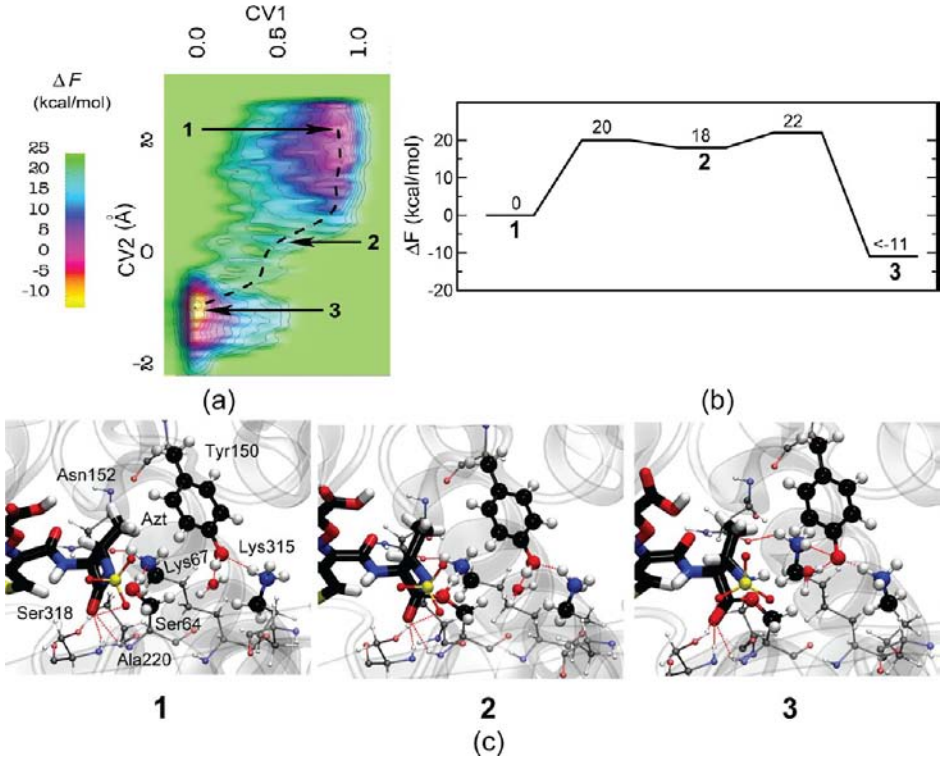

Figure 5. (a) Reconstructed free energy surface, (b) free energy profile, and (c) snapshots for the acylation reaction of CBL with aztreonam. In (a), the dotted line is the sketch of the minimum energy pathway. CV1 and CV2 correspond to the collective variables coupled to CC1 and CC2, respectively; see the text. The minimum **3** was not completely sampled; therefore, the exact relative free energy of **3** was not determined. The depth of **2** was estimated in an independent metadynamics simulation; see Supporting Information section 9.

To acquire confidence in the saddle point obtained, we have carried out transition path sampling (TPS) simulations.[59] The results of these simulations are given in Supporting Information section 4. These results show that the transition-state structures obtained from the metadynamics simulation are indeed close to the true saddle point and also confirm the presence of the intermediate **5** as represented on the free energy surface. However, it is noted in passing that the above experiments do not guarantee that there exits another set of coordinates for which a pathway with lower free energy can be obtained. Usually a refinement procedure like the one in ref 60 would indicate the involvement of other slow coordinates, but is computationally unaffordable for this work.

Another source of error in the free energy estimates is the PBE functional used in our calculations. We have carried out error analysis of the functional and found that the PBE functional introduces errors of about +1.4 to −2.7 kcal mol^{-1} in comparison with the M06-2X functional;[61] see Supporting Information section 5. A similar error estimate for the PBE functional was also seen in our previous study.[28] Furthermore, a ±2 kcal mol^{-1} error in the free energy estimates is expected due to the metadynamics technique.[62]

3. RESULTS AND DISCUSSION

3.1. Equilibrium Structures of Henry−Michaelis Complexes. Equilibrium structures of the noncovalent complex formed by the drug molecules and the CBL were obtained through classical force-field-based MD simulations.

3.1.1. CBL−Aztreonam Complex. Two independent classical simulations were performed starting with aztreonam precomplexed structures in the **K$^+$Y$^-$:Azt** and **KY:Azt** protonation states (Figure 2). The maximum RMSD plots of the protein backbone for **K$^+$Y$^-$:Azt** and **KY:Azt** reflect the stability of these structures (see Figure SI 5, Supporting Information).

The equilibrated **KY:Azt** is characterized by a stable $Ser_{64}O_\gamma$ contact with $Lys_{67}N_\zeta$ (d[$Ser_{64}O_\gamma\cdots Lys_{67}N_\zeta$] = 2.74 ± 0.14 Å); see Figure 4. During the simulation of **KY:Azt**, we could characterize two different conformations of the active site, namely, KY:AztA and KY:AztB. The major differences between these two structures are in the interaction of Lys_{67} with Asn_{152} and Ala_{220} and the relative positions of Lys_{67} and Tyr_{150}. In KY:AztA, $Lys_{67}H_\zeta$ interacts with both $Asn_{152}O_\delta$ and $Ala_{220}O$ and the average distance between the $Lys_{67}N_\zeta$ and $Tyr_{150}O_\eta$ side chains is 4.53 ± 0.39 Å. On the other hand, in KY:AztB, $Lys_{67}N_\zeta$ interacts only with $Asn_{152}O_\delta$ and the average distance between the $Lys_{67}N_\zeta$ and $Tyr_{150}O_\eta$ side chains is 3.76 ± 0.31 Å; see also Figure SI 6, Supporting Information. In both configurations, Tyr_{150} is hydrogen bonded[63] with a water molecule throughout the simulation, with the former being the hydrogen bond donor. The hydroxyl group of Ser_{64} is hydrogen bonded with the side chain of Lys_{67}, and no interaction was observed between Lys_{67} and Tyr_{150}.

In the case of the **K$^+$Y$^-$:Azt** protonation state (Figure 4 ; Table SI 3, Supporting Information), Tyr_{150} is hydrogen bonded to Lys_{315} and Lys_{67} (d[$Tyr_{150}O_\eta\cdots Lys_{315}N_\zeta$] = 2.85 ± 0.11 Å and d[$Tyr_{150}O_\eta\cdots Lys_{67}N_\zeta$] = 2.91 ± 0.17 Å). Despite the anionic state of Tyr_{150}, we observed some transient structures in the trajectory where $Ser_{64}H_\gamma$ interacted with $Tyr_{150}O_\eta$. The $Ser_{64}H_\gamma\cdots Azt_{362}O_9$ contact (d[$Ser_{64}H_\gamma\cdots Azt_{362}O_9$] = 2.23 ± 0.44 Å) was preserved through most of the simulation.

Interestingly, **KY:Azt** and **K$^+$Y$^-$:Azt** structures resemble well the precomplexed active site structure reported by Díaz et al.[26] and the apoenzyme active site structure reported by us.[28] In these structures, the aztreonam carbonyl group is well situated in the oxyanion hole created by Ser_{64}NH and Ser_{318}NH. Moreover, the sulfonyl group of aztreonam is hydrogen bonded

dx.doi.org/10.1021/ja405319n | J. Am. Chem. Soc. 2013, 135, 14679−14690

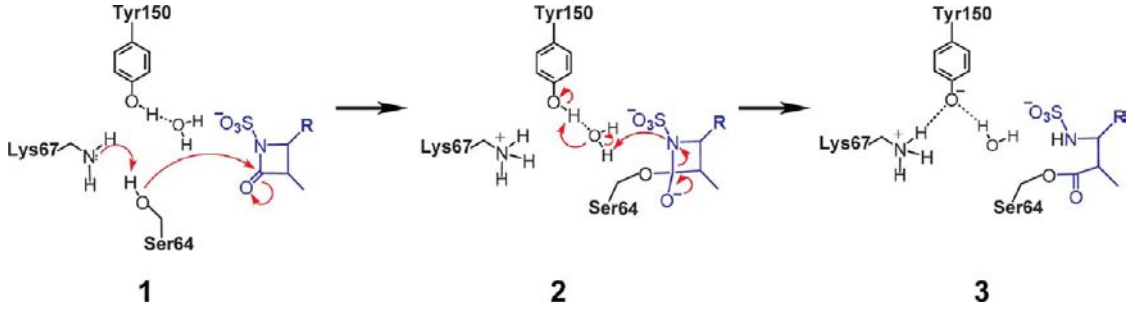

Figure 6. Mechanism of the acylation reaction of CBL with aztreonam as obtained from our simulations. See also Figure 5.

to the ammonium group of Asn_{346} and the hydroxyl group of Ser_{318}. Here, $Ser_{64}O_\gamma$ is in a good position to attack aztreonam C_2 (based on their distance); see Figure 4 and Table SI 3, Supporting Information.

3.1.2. CBL−Cephalothin Complex. The results of the empirical force field MD simulation of class C β-lactamase with cephalothin substrate have been discussed in detail in our previous paper.[28] In the stable conformer **KY:Cep**, $Ser_{64}H_\gamma$ points toward the carboxylate group of Cep_{362} and Tyr_{150} interacts directly with Lys_{67}. In the other protonation state, **K^+Y^-:Cep**, $Ser_{64}H_\gamma$ interacts with the carboxylate group of Cep_{362} and $Lys_{67}H_\zeta$ interacts with both $Tyr_{150}O_\eta$ and $Ser_{64}O_\gamma$. For more details see Figure 4 and Table SI 3, Supporting Information.

3.2. CBL−Aztreonam Acylation Reaction: Mechanism and Free Energies. Free energy calculations by Díaz et al.[26] showed that **KY:Azt** is ∼20 kcal mol^{-1} lower in free energy compared to **K^+Y^-:Azt**. Weak interactions of Ser_{64} with other base residues in **K^+Y^-:Azt** make it less favorable for the acylation reaction in comparison with **KY:Azt**, where Ser_{64} remains in a good position to delocalize its proton to Lys_{67}. On the basis of these facts, we concluded that **KY:Azt** would be a good starting structure for the acylation reaction. From the arbitrarily chosen structure of the solvated aztreonam−enzyme complex KY:AztB, we carried out a QM/MM metadynamics simulation to explore the acylation reaction. We chose two CCs for this purpose: (a) the coordination number of $Ser_{64}O_\gamma$ to $Ser_{64}H_\gamma$, $Lys_{67}H_\zeta$, and $Tyr_{150}H_\eta$ (CC1) and (b) the distance difference $d[Ser_{64}O_\gamma{-}Azt_{362}C_2] - d[Azt_{362}C_2{-}Azt_{362}N_1]$ (CC2). CC1 was selected to accelerate the proton transfer from $Ser_{64}O_\gamma$ to any base, and CC2 is for sampling the nucleophilic attack of $Ser_{64}O_\gamma$ on $Azt_{362}C_2$ and the breaking of the $Azt_{362}C_2{-}Azt_{362}N_1$ bond. The value of CC1 changes from ∼1 to ∼0 when a base takes a proton from Ser_{64}, and CC2 changes from ∼+2 to ∼−2 Å on the attack of $Ser_{64}O_\gamma$ on $Azt_{362}C_2$ followed by the breaking of the $Azt_{362}C_2{-}Azt_{362}N_1$ bond. A wall potential was applied at 2.65 Å along CC2 to avoid sampling the unbound states of the drug molecule. We emphasize that the collective coordinates chosen here do not assume any particular residue as the base, and therefore, the current simulation will be able to predict which among the active site residues will act as a general base. Furthermore, we have not specifically included the coordinates for the proton transfer to $Azt_{362}N_1$, and thus, this may take place (as a result of the breaking of the $Azt_{362}C_2{-}Azt_{362}N_1$ bond which was sampled explicitly) along the minimum energy route.

Using these coordinates, we were able to simulate the acylation reaction. The reconstructed free energy surface of the acylation reaction is shown in Figure 5. The net free energy barrier for this process is calculated to be 22 kcal mol^{-1}. The reaction from **1** to **3** proceeds through the intermediate **2**. The free energy barriers for **2** → **1** and **2** → **3** are 2 and 4 kcal mol^{-1}, respectively. The free energy barrier for **2** → **1** was estimated by another metadynamics simulation, whose details are given in Supporting Information section 9.

On analyzing the trajectory, we could dissect the detailed mechanism of the acylation reaction; see Figure 6. Proton transfer from $Ser_{64}O_\gamma$ to $Lys_{67}N_\zeta$ has occurred first, followed by the formation of a $Ser_{64}O_\gamma{-}Azt_{362}C_2$ bond. The $Azt_{362}C_2{-}Azt_{362}N_1$ bond is elongated but not completely cleaved in the intermediate structure **2**. Ensuing this, the water molecule which is hydrogen bonded with the $Tyr_{150}H_\eta$ reorients toward $Azt_{362}N_1$ and the proton shuttles from Tyr_{150} to $Azt_{362}N_1$ through the bridging water molecule. This is concomitant with the cleavage of the $Azt_{362}C_2{-}Azt_{362}N_1$ bond. On further carrying out these QM/MM calculations, we observed the formation of hydrogen bond interactions between Lys_{67} and Tyr_{150}, in agreement with the X-ray structure.[24] See also the movie of the reactive trajectory (starting near the first barrier crossing) in the Supporting Information.

To further verify the possibility of Tyr_{150} as a base, we carried out simulations starting from the **K^+Y^-:Azt** state; see Supporting Information section 11. During the simulations, we observed that, when a full proton transfer occurs from Ser_{64} to Tyr_{150}, one of the Lys_{67} protons transfers to Ser_{64}, thus giving the **KY:Azt** protonated structure. Then we restricted the protonation state of Lys_{67} to sample only the reaction pathway with Tyr_{150} as the base. It was found that the acylation reaction does not take place even after a free energy of 38 kcal mol^{-1} is reached, which is much larger than the free energy barrier along the route where Lys_{67} activates Ser_{64}. On the basis of this result, we can exclude the possibility of Tyr_{150} acting as the base for the acylation of aztreonam.

We also carried out a metadynamics simulation starting with the KY:AztA conformer (see Supporting Information section 12). In this case, the free energy barrier for the acylation reaction was found to be >25 kcal mol^{-1}. The reason for this high barrier, compared to that with the KY:AztB conformer, can be attributed to the difference in the relative positions of Tyr_{150} with respect to Lys_{67}. In KY:AztA, Tyr_{150} remains far from Lys_{67} ($d[Lys_{67}N_\zeta{\cdots}Tyr_{150}O_\eta]$ = 4.53 Å) and thus weakly stabilizes the cationic Lys_{67} formed after the withdrawal of the Ser_{64} proton, unlike in the KY:AztB conformer, where Tyr_{150} is in a suitable orientation to stabilize the cationic Lys_{67}.

It is interesting to note that KY:AztB does deviate from the X-ray structure,[24] especially in the $Ala_{220}{\cdots}Lys_{67}$ interaction, but has a lower free energy barrier for the acylation reaction compared to KY:AztA. Therefore, it is concievable that the active site adapts to the KY:AztB state from its preferred KY:AztA state during the reaction, especially because the

dx.doi.org/10.1021/ja405319n | J. Am. Chem. Soc. 2013, 135, 14679−14690

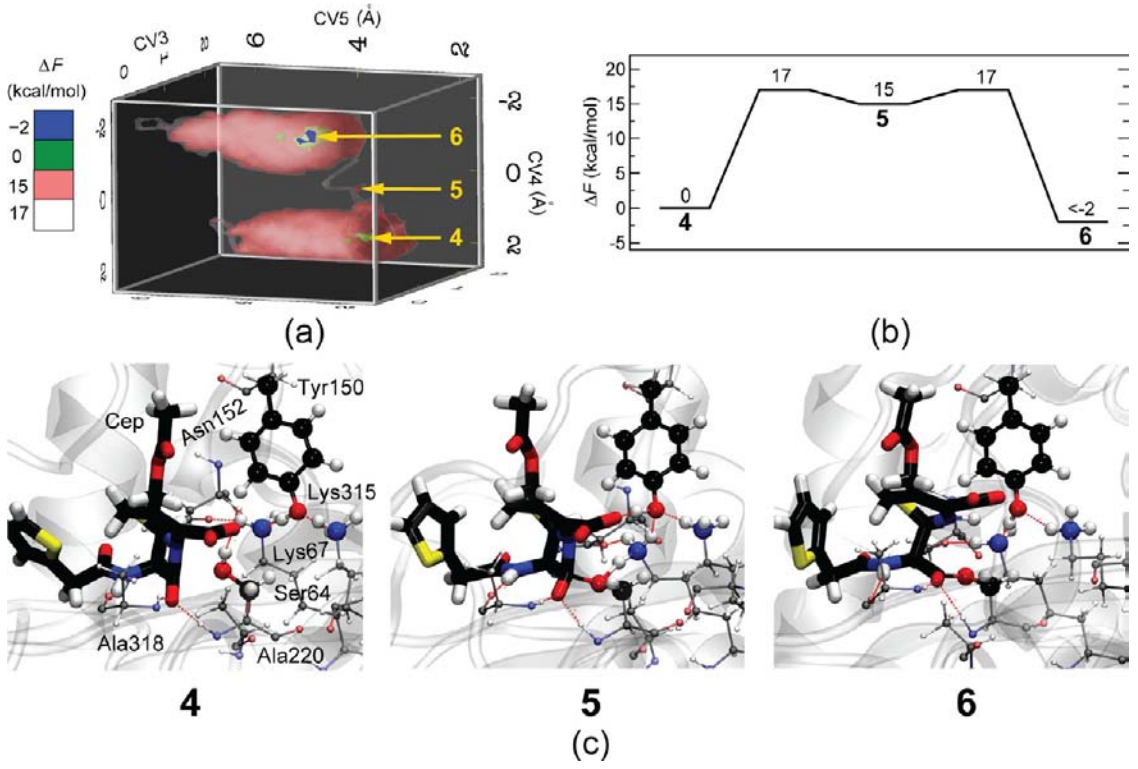

Figure 7. (a) Reconstructed free energy surface, (b) free energy profile, and (c) snapshots for the acylation reaction of CBL with cephalothin. In (a) the free energy surface is visualized as three-dimensional contour surfaces for various isovalues. CV3, CV4, and CV5 correspond to the collective variables coupled to CC3, CC4, and CC5, respectively; see the text. The minimum **6** was not completely sampled, and therefore, the exact relative free energy of **6** was not determined. The depth of the intermediate **5** was estimated in an independent metadynamics simulation; see Supporting Information section 10.

conversion KY:AztA → KY:AztB is faster than the acylation reaction (section 3.1.1). Thus, we propose that the $Ala_{220}\cdots Lys_{67}$ interaction breaks during the acylation reaction. This interaction may be re-formed after the formation of the acylated complex as observed in the X-ray structure.

3.3. CBL−Cephalothin Acylation Reaction: Mechanism and Free Energies. To explore the full acylation path of the cephalothin substrate, a metadynamics simulation was performed with the **KY:Cep** protonation structure. We chose three CCs for this simulation: (a) the coordination number of $Ser_{64}O_\gamma$ to $Ser_{64}H_\gamma$, $Lys_{67}H_\zeta$, and $Tyr_{150}H_\eta$ (CC3), (b) the distance difference $d[Ser_{64}O_\gamma - Cep_{362}C_8] - d[Cep_{362}C_8 - Cep_{362}N_5]$ (CC4), and (c) the distance of $Ser_{64}O_\gamma$ to $Lys_{67}N_\zeta$ (CC5). The first two CVs were similar to CC1 and CC2, as considered in the previous simulation. CC5 was chosen for sampling different relative orientations of Lys_{67} with Ser_{64}; preliminary metadynamics simulations (data not shown) indicated that this coordinate is crucial to explore the possibility of the carboxylate group as a general base. Mainly, when the carboxylate group took the proton from $Ser_{64}O_\gamma$, we observed a spontaneous proton transfer from $Lys_{67}N_\zeta$ to $Ser_{64}O_\gamma$. This was possible because Tyr_{150} simultaneously transferred a proton to the neutral $Lys_{67}N_\zeta$. This prevented $Ser_{64}O_\gamma$ from further attacking $Cep_{362}C_8$. Using CC5, we sampled configurations where $Lys_{67}N_\zeta$ is far from $Ser_{64}O_\gamma$ during the proton transfer to the carboxylate. This was not an issue in the case of aztreonam, as there are no carboxylate groups present, and moreover, the neutral Lys_{67} entity is not hydrogen bonded to Tyr_{150} and therefore cannot act as a proton donor. A wall potential was placed along CC4 at +2 Å to avoid sampling drug-unbound states. The value of CC3 changes from ∼1 to ∼0 when Ser_{64} gives its proton to a base, and CC4 changes from ∼+2 to ∼−2 on the formation of the $Ser_{64}O-Cep_{362}C_8$ bond and the breakage of the $Cep_{362}C_8-Cep_{362}N_5$ bond.

The reconstructed free energy surface after the simulation of the reaction is shown in Figure 7. The effective free energy barrier for **4** → **6** is 17 kcal mol^{-1}. An intermediate **5** was also observed like before. The free energy barrier for **5** → **4** is only 2 kcal mol^{-1} and was obtained from a separate metadynamics simulation; see Supporting Information section 10.

This metadynamics simulation also sampled both the protonation states **KY:Cep** and $\mathbf{K^+Y^-}$**:Cep** due to the low free energy barrier separating them;[28] see also Figure SI 13, Supporting Information. We observed transfer of $Ser_{64}H_\gamma$ to the carboxylate group of the drug, $Tyr_{150}O_\eta$ (in the $\mathbf{K^+Y^-}$**:Cep** state) and $Lys_{67}N_\zeta$, during the metadynamics simulation; see Figure SI 14, Supporting Information. However, the proton transfers from $Ser_{64}O_\gamma$ to the carboxylate and $Tyr_{150}O_\eta$ did not lead to the acylated intermediate. Along the minimum energy pathway connecting the reactant state to the acylated product state, from **4** to **6**, we observed proton transfer from $Ser_{64}O_\gamma$ to $Lys_{67}N_\zeta$ subsequent to the breakage of the $Ser_{64}H_\gamma$ interaction with the carboxylate group of the drug molecule. Interestingly, this structure resembles very well the short-lived structure seen in the classical force field simulation.[28] Subsequently, a proton transfer occurred from Ser_{64} to Lys_{67}, with a simultaneous attack of $Ser_{64}O_\gamma$ on $Cep_{362}C_8$. These processes resulted in the formation of the intermediate **5**. In the following steps of the reaction, the β-lactam ring opened and protonation of the $Cep_{362}N$ occurred. The carboxylate group of Cep_{362} abstracted a proton from Tyr_{150}, which reoriented and hydrogen bonded with Cep_{362} after the rotation of Ser_{64} toward Lys_{67}, and

dx.doi.org/10.1021/ja405319n | J. Am. Chem. Soc. 2013, 135, 14679−14690

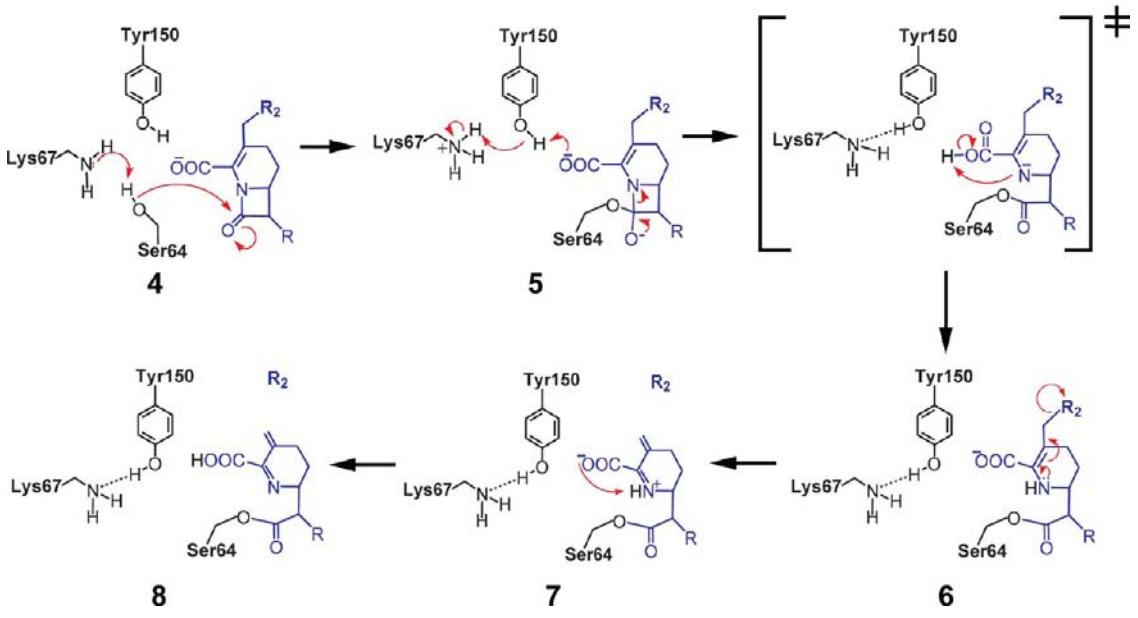

Figure 8. Mechanism of the acylation reaction between CBL and cephalothin and the subsequent R_2 group release. For cephalothin, the R_2 group is the acetate anion. See also Figures 7 and 9.

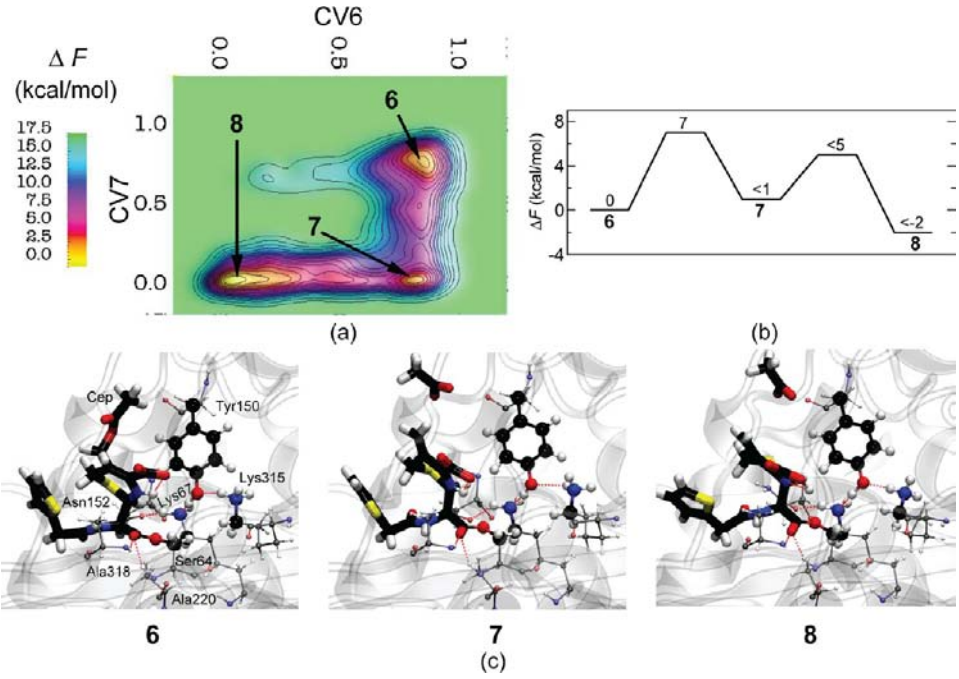

Figure 9. (a) Reconstructed free energy surface, (b) free energy profile, and (c) snapshots during the R_2 group (acetate anion) release from the CBL−cephalothin acylated complex. See also Figure 8. CV6 and CV7 are the collective variables corresponding to the collective coordinates CC6 and CC7, respectively. The exact free energy difference between **7** and **6** was not obtained as **7** was not fully sampled. The free energy barriers for **7** → **8** and **8** → **7** have been measured from the simulation and are 4 and 7 kcal mol^{-1}, respectively.

subsequently transferred it to $Cep_{362}N_5$. In the case of aztreonam, which lacked the carboxylate group, a water molecule was used as the proton transfer agent (from $Tyr_{150}O_\eta$ to the N of the lactam drug). The above protonation step completes the breakage of the $Cep_{362}C_8$−$Cep_{362}N_5$ bond; see Figure 8. We again stress the fact that no CCs were explicitly taken for the proton transfer process, and this occurred spontaneously due to the sampling of other coordinates. In the product state, the protonated Lys_{67} is hydrogen bonded with Tyr_{150}, and frequent proton transfer occurs between the two residues. A movie of this reactive trajectory (starting near the first barrier crossing) is available in the Supporting Information.

In the crystal structure of the acylated enzyme,[25] the acetate anion R_2 group is found released from the substrate. To validate the R_2 group exit mechanism, another metadynamics simulation was initiated with the acylated structure **6** as obtained from the previous metadynamics simulation. Two CCs have been chosen for this simulation: (a) the coordination number of $Cep_{362}C_{3'}$ to $Cep_{362}O_{20}$ (CC6) and (b) the coordination number of

dx.doi.org/10.1021/ja405319n | J. Am. Chem. Soc. 2013, 135, 14679−14690

$Cep_{362}N_5$ to the hydrogen bound to $Cep_{362}N_5$ and three hydrogen atoms of $Lys_{67}N_\zeta$ (CC7). CC6 was chosen to accelerate the breakage of the $Cep_{362}C_{3'}$−$Cep_{362}O_{20}$ bond, and CC7 was chosen for accelerating the deprotonation of $Cep_{362}N_5$ (to verify that a proton transfer from $Cep_{362}N_5$ to the carboxylate group can assist the R_2 group exit).

The reconstructed free energy surface for the R_2 release is shown in Figure 9. Three minima can be observed in this reconstructed free energy surface. The free energy barrier to reach structure **7** through the breakage of the $Cep_{362}C_{3'}$−$Cep_{362}0_{20}$ bond without deprotonation of $Cep_{362}N_5$ is about 7 kcal mol^{-1}; see also Figure 8. We observed a retro-Michaels addition mechanism for the R_2 release. Proton transfer from $Cep_{362}N_5$ to the carboxylate group of Cep_{362} was also observed (i.e., formation of **8**). However, the R_2 exit process does not require this to occur; see the minimum energy pathway in Figure 9. The free energy barrier for this proton transfer (**7** → **8**) is about 4 kcal mol^{-1}, while the reverse barrier (**8** → **7**) for the protonation state is 7 kcal mol^{-1}. During the R_2 release, we observed a rotation of the substrate about the C_6−C_7 bond by about 45°. Interestingly, we have also observed the diffusion of a water molecule toward the active site after the R_2 release. The R_2 release is a relatively fast process compared to acylation, and crucially, it makes the acylation process irreversible by dissociating the R_2 group.

3.4. Discussion. *3.4.1. General Base for Activating Ser_{64}.* Simulations were carried out in such a way that a general base was not explicitly defined in the CCs, while they were able to identify the general base for acylation without any specific inputs based on chemical intuitions. We found that Lys_{67} acts as the base during the acylation, independent of the drug molecule and the protonation state of Lys_{67} and Tyr_{150} in the starting structure. Simulations which specifically modeled Tyr_{150} as the base showed that such a reaction route is not energetically preferred. Moreover, our metadynamics simulation with cephalothin sampled $Ser_{64}H_\gamma$ transfer to the carboxylate group of the drug, as well as to $Tyr_{150}O_\eta$, and did not lead to the formation of the acyl−enzyme complex. It may also be noticed that prediction of the reaction mechanism based on the interactions in the equilibrium reactant structure may not always be conclusive.

Our proposed mechanism is in complete agreement with that proposed by Dubus et al.[22] where Lys_{67} is considered as a general base. A similar mechanism was also proposed for the acylation mechanism in PBPs.[64] On the basis of the interactions between $Tyr_{150}O_\eta$ and the carboxylate group of Cep_{362} in the crystallographic precomplexed structure (having an S64G mutation), Shoichet and his group[25] proposed a mechanism where a proton transfer initially occurs from Tyr_{150} to Cep_{362} and the former in turn activates Ser_{64}. Although our simulations (where a wild type is used instead of the S64G mutation) do not agree with this, and in particular the Cep_{362}···Tyr_{150} interaction was not seen in the equilibrium trajectories of our simulation, we observed transient structures with the Cep_{362}··· Tyr_{150} interaction after the rotation of Ser_{64} toward Lys_{67}, in agreement with their reported crystal structure. Chen et al.[30] reported a significant change in the values of k_{cat} and k_{cat}/K_m after the K67R mutation with cephalothin as the drug molecule. On the basis of this study, they proposed a conjugate base mechanism where Lys_{67} activates Ser_{64} and the proton transfer to Cep takes place through the route Lys_{67} → Tyr_{150} → Cep. This mechanism agrees with the fact that Lys_{67} acts as the base; however, we observed a different proton transfer mechanism from Lys. MD simulations by Díaz et al.[26] also proposed Lys_{67} as a base during the acylation of aztreonam.

On the basis of the conjecture that the anionic phenolate form of Tyr_{150} is present in the active site, this residue has been proposed as the general base by many.[17,24,29,31−34,65] This is ruled out by our studies. Our study also clearly refutes the possibility of a drug molecule as the general base during the acylation.[37]

We are also proposing here that the Ala_{220}···Lys_{67} interaction breaks before the acylation. We found that the presence of this interaction keeps the Lys_{67} far from Tyr_{150} in the noncovalent complex, resulting in a higher free energy barrier for acylation. Although this interaction is present in the crystal structures of several acylated complexes, a distance of 4.35 (3.6) Å between them in chain B (A) of 1FR6 (PDB)[24] is in agreement with our proposal. There are a few other crystal structures of acylated complexes where the Ala_{220}···Lys_{67} contact is absent, e.g., 1FR6 (4.35 Å in chain B),[24] 2Q9M (4.59 Å),[66] 1O07 (5.33 Å),[67] 1FCM (5.05 Å),[34] and 1I5Q (4.81 Å).[68] It is likely that this interaction is re-formed after the acylation, but future calculations may verify this. Since the mechanisms of formation of the tetrahedral complex in KY:AztA, KY:AztB, and **KY:Cep** are the same, we can also conclude that the mechanism is independent of the Ala_{220}···Lys_{67} interaction.

3.4.2. Mechanism of Protonation of the β-Lactam Ring. Protonation of the ring is a necessity for the complete ring-opening process. Various mechanisms may operate in the protonation of the N of the β-lactam ring during the acylation. In our simulations, no explicit coordinates were used to sample this event; however, we observed it to be spontaneous after the ring-opening step in the acylation. Therefore, the mechanism observed for this process is not biased by any chemical intuitions used in the selection of CCs.

It is shown here that the protonation of N occurs after the proton transfer from Ser_{64} to Lys_{67} and the formation of the C−$SerO_\gamma$ bond. Importantly, an intermediate is formed before the protonation of N, where d[C−N] ≈ 1.58 Å and d[C−$SerO_\gamma$] ≈ 1.61 Å. We observed that Tyr_{150} has the role of protonating N, and it occurs through a proton relay mechanism. Interestingly, for both the substrates, Tyr_{150} does not directly donate its proton to the lactam N; instead, it is transferred through a water molecule in the case of aztreonam while it is mediated by the carboxylate group in the case of cephalothin.

Although there is a difference in the detailed mechanisms for these drugs, a cooperative role of Lys_{67} and Tyr_{150} in transferring the proton seems common to both. The solvent-mediated proton transfer mechanism detected in the case of aztreonam could be generalized for other monobactams, as this subclass of antibiotics lack the bicyclic core with a carboxylate functional group. Similarly, the substrate-mediated proton transfer mechanism could be active in all cephalosporin antibiotics. We note here in passing that this conclusion has to be further verified for penams and other subclasses of drugs as the carboxylate group can have different relative orientations.[69]

Our findings are in line with the mechanism envisaged by Dubus et al.,[22] where Lys_{67} activates Ser_{64} and Tyr_{150} has the role of protonating the lactam N. Moreover, Chen et al.[30] have conjectured a similar proton transfer from the general base Lys_{67} to the substrate through Tyr_{150}, but via a direct proton transfer to N from Tyr_{150}.

3.4.3. Comparison with Experimental Data. We mentioned earlier that it is difficult to trace the acylation reaction through experiments, as this reaction is relatively fast, and the only accessible information is the rate constant (k_2) for the acylation reaction and the crystallographic structures of the acylated product in some cases. For aztreonam, the value of k_2 is reported to be >150 s^{-1},[12] which corresponds to a free energy barrier of <15 kcal mol^{-1}. For cephalothin, we are not aware of any reported k_2 values; however, for cefotaxime (which also belongs to the cephalosporin subfamily), it is also reported to be >150 s^{-1} by the same authors.[12] Therefore, the free energy barrier estimates from the experiments do not differentiate these two drugs (both <15 kcal mol^{-1}). The estimated k_2 values for various other penem and cephem drug molecules correspond to the free energy barriers in the range of 15−17 kcal mol^{-1}.[12,23] Therefore, our free energy estimate of 17 kcal mol^{-1} for cephalothin is in reasonably good agreement with the experimental data. The free energy barrier for the acylation of aztreonam is 7 kcal mol^{-1} higher than that from the experiments and 5 kcal mol^{-1} higher than that for cephalothin.

The origin of the differential reactivity between the drugs could be ascribed to the difference in the distance between Lys_{67} and Tyr_{150} and the orientation of Ser_{64} with respect to Lys_{67}. In the case of cephalothin, interactions between the carboxylate group and Ser_{64} favor the hydrogen-bonding interaction between Lys_{67} and Tyr_{150}. On the other hand, due to a lack of hydrogen-bonding interactions between Ser_{64} and aztreonam, Ser_{64} orients toward Lys_{67}, and that destabilizes the hydrogen-bonding interactions between Lys_{67} and Tyr_{150}. In fact, during the equilibrium classical force field simulations of the noncovalent complex, no hydrogen-bonding interaction was noticed between Lys_{67} and Tyr_{150}, although this interaction was present in the initial configuration. The absence of the $Lys_{67}\cdots Tyr_{150}$ interaction was also observed by Díaz et al.[26] in their simulation of the aztreonam−enzyme Michaelis complex. It is very important to note here that, in all the simulations, the Lys_{67} and Tyr_{150} interaction is re-formed after the acylation of aztreonam. This is because Lys_{67} loses its interaction with Ser_{64} during the acylation reaction when the latter forms a covalent bond with the drug. The presence of $Lys_{67}\cdots Tyr_{150}$ interactions in the product is in agreement with the crystal structure of the acylated complex.[24] As no precomplexed PDB structures of CBL are available with aztreonam, a direct comparison of **KY:Azt** with the experiments is difficult. The same arguments as above can also explain the presence of $Lys_{67}\cdots Tyr_{150}$ interactions in the transition-state analogue 2FFY,[36] where Ser_{64} does not have contact with Lys_{67} since Ser_{64} is covalently bound to the boron substrate. In the case of cephalothin, the formation of charged Lys_{67} is better stabilized in the course of the acylation due to its interaction with $Tyr_{150}O_{\eta}$ compared to the case of aztreonam, where these residues do not form direct contacts. The origin of this difference can also be due to the artifacts of limited sampling and empirical force field parameters. We expect that these could only result in overestimating the free energy barriers and not the mechanism of acylation, since the presence of the $Lys_{67}\cdots Tyr_{150}$ interaction is shown to not affect the mechanism of the formation of the tetrahedral intermediate.

A direct comparison between the structure of the acylated product obtained from our metadynamics simulations and the X-ray structure is not straightforward. The QM/MM metadynamics trajectory of the acylated complex is only obtained for a less than 3 ps time scale (in the product minimum), which may not be sufficient to relax the active site structure to equilibrium. Thus, further simulations are required to look into the equilibrium structure of the acylated complex. However, many striking similarities can be observed between the acylated structure from X-ray and the simulations. As seen in the crystallographic structure[25] of cephalothin, we too noticed a rotation of the acylated drug molecule about the C_6-C_7 bond, resulting in the diffusion of the deacylating water close to O_9; see Figure 10. Differences have been found,

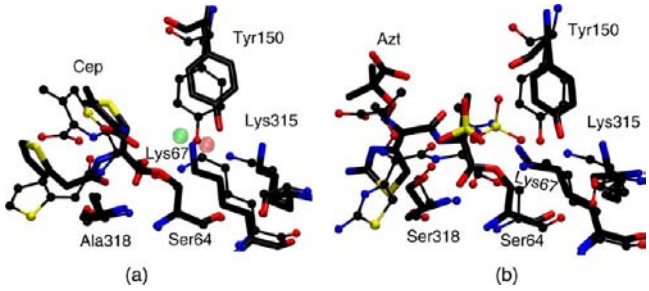

Figure 10. (a) Average active site structure of the cephalothin−CBL acyl−enzyme complex from simulation (licorice style) overlapped with the X-ray structure[25] (CPK, Corey−Pauling−Koltun) and (b) snapshot of the aztreonam−CBL acyl−enzyme complex from simulation (licorice style) overlapped with the X-ray structure[24] (CPK). In (a) the deacylating water seen in the X-ray (green transparent sphere) and in the simulation (red transparent sphere) is also highlighted.

however, in the puckering of the six-membered ring dihydrothiazine and the carboxylate group interaction with Asn_{343}. Importantly, O_9 is not located in the oxyanion hole in the crystal structure, while it is retained in our simulation, and no rotation about $Ser_{64}O_{\gamma}-C_8$ bond is observed. Similarly, the acyl−enzyme complex formed by aztreonam in the simulations showed interactions of deprotonated Tyr_{150} with both Lys_{67} and Lys_{315}, similar to the X-ray structure;[24] see Figure 10. Interestingly, the $Tyr_{150}\cdots Lys_{67}$ interaction, which was absent during the acylation reaction of aztreonam, re-forms after the formation of the acyl−enzyme complex. Interaction of the SO_3^- group with Lys_{315} seen in the X-ray structure was not observed in our simulations, in line with the results of Díaz et al.[26]

4. SUMMARY AND CONCLUSION

Through extensive QM/MM metadynamics simulations, we have unraveled the detailed mechanism of the formation of the acyl−enzyme complex from the Henry−Michaelis complex of a β-lactam antibiotic and class C β-lactamase and addressed the outstanding questions regarding the reaction mechanism. To verify if the mechanism is drug independent, we have simulated the acylation reaction with aztreonam and cephalothin drugs belonging to the cephalosporin and monobactam subclasses, respectively. We identified that the general base involved in the acylation of the drug is Lys_{67} for both the drugs. Proton transfer to Tyr_{150} and the drug carboxylate group does not lead to the acylation reaction, and thus, these residues are ruled out as the general base.

Acylation of drugs happens through a two-step process: (a) formation of a tetrahedral intermediate; (b) proton transfer to the lactam N occurring from Tyr_{150}. We found that the proton transfer from Tyr_{150} to the lactam N occurs through a water bridge in the case of aztreonam and via the substrate

dx.doi.org/10.1021/ja405319n | J. Am. Chem. Soc. 2013, 135, 14679−14690

carboxylate group in the case of cephalothin. The R_2 group release which proceeds through a retro-Michael reaction is much faster than the acylation reaction of cephalothin. The free energy barrier estimated for the acylation reaction for cephalothin is quantitatively close to the experimental estimate, while it differs for the case of aztreonam. We have observed a slower acylation of aztreonam compared to cephalothin, which is traced back to the relative orientation of the active site residues as a result of the carboxylate group present in cephalothin. On the basis of the observation that the $Ala_{220}\cdots Lys_{67}$ interaction keeps the Lys_{67} far from Tyr_{150} in the noncovalent complex, thus resulting in a higher free energy barrier for acylation than the case where this interaction is absent, we are proposing that the $Ala_{220}\cdots Lys_{67}$ interaction breaks before acylation and might re-form after the reaction.

We believe that the molecular details of the mechanism will greatly help to understand the antibiotic resistance in class C β-lactamases. In fact, tailoring drug/inhibitor molecules to make the acylation step reversible is a viable strategy to increase the efficiency of drugs.[70] Thus, the results of this work could aid in the design of novel drugs and inhibitors with improved resistance to class C β-lactamases.

■ ASSOCIATED CONTENT

Supporting Information

(a) Simulation details, (b) detailed error analysis, (c) RMSD plot, (d) structural data of various protonation states, (e) metadynamics simulations (**2**→ **1**, **5** → **4**, acylation reaction with **K^+Y^-:Azt** with Tyr_{150} constrained as a base, and acylation starting with the **KY:Cep** structure), (f) various configurations observed during acylation reaction of cephalothin, (g) PDB file with coordinates of the reactants, transition states, and products (seen immediately after the acylation), and (h) movie (mpg) files showing the acylation reactions in aztreonam−CBL and cephalothin−CBL complexes. This material is available free of charge via the Internet at http://pubs.acs.org.

■ AUTHOR INFORMATION

Corresponding Author

nnair@iitk.ac.in

Notes

The authors declare no competing financial interest.

■ ACKNOWLEDGMENTS

Part of the calculations were performed using the computer cluster installed at the Department of Chemistry, Indian Institute of Technology Kanpur (IIT Kanpur), through the Department of Science & Technology's Fund for Improvement of S&T Infrastructure in Higher Educational Institutions (DST-FIST) program and using the High Performance Computing (HPC) facility at IIT Kanpur. R.T. acknowledges the Council of Scientific and Industrial Research (CSIR), India, for a fellowship. N.N.N. also acknowledges Dr. Ramesh Ramapanicker (IIT Kanpur) for helpful discussions on the retro-Michael addition reaction.

■ REFERENCES

(1) Waxman, D. J.; Strominger, J. L. *Annu. Rev. Biochem.* **1983**, *52*, 825−869.
(2) Livermore, D. M. *Clin. Microbiol. Rev.* **1995**, *8*, 557−584.
(3) Palzkill, T. G.; Majiduddin, F. K.; Materon, I. C. *Int. J. Med. Microbiol.* **2002**, *292*, 127.
(4) Beceiro, A.; Bou, G. *Rev. Med. Microbiol.* **2004**, *15*, 141−152.
(5) Fisher, J. F.; Meroueh, S. O.; Mobashery, S. *Chem. Rev.* **2005**, *105*, 395−424.
(6) Ambler, R. P. *Philos. Trans. R. Soc. London, B* **1980**, *289*, 321.
(7) Nicolas-Chanoine, M. H. *Int. J. Antimicrob. Agents* **1996**, *70*, S21−S26.
(8) Gransden, W. R. *J. Med. Microbiol.* **1997**, *46*, 436−439.
(9) Peleg, A. Y.; Hooper, D. C. *N. Engl. J. Med.* **2010**, *362*, 1804−1813.
(10) Paterson, D. L.; Bonomo, R. A. *Clin. Microbiol. Rev.* **2005**, *18*, 657−686.
(11) Majiduddin, F. K.; Materon, I. C.; Palzkill, T. G. *Int. J. Med. Microbiol.* **2002**, *292*, 127−137.
(12) Monnaie, D.; Dubus, A.; Frère, J.-M. *Biochem. J.* **1994**, *302*, 1−4.
(13) Cavalli, A.; Carloni, P.; Recanatini, M. *Chem. Rev.* **2005**, *106*, 3497−3519.
(14) Fenollar-Ferrer, C.; Frau, J.; Donoso, J.; Muñoz, F. *Theor. Chem. Acc.* **2008**, *121*, 209−218.
(15) Pratt, R. F. *Science* **1989**, *246*, 917−919.
(16) Nukaga, M.; Haruta, S.; Tanimoto, K.; Kogure, K.; Taniguchi, K.; Tamaki, M.; Sawai, T. *J. Biol. Chem.* **1995**, *270*, 5729−5735.
(17) Powers, R. A.; Shoichet, B. K. *J. Med. Chem.* **2002**, *45*, 3222−3234.
(18) Rahil, J.; Pratt, R. F. *Biochemistry* **1992**, *31*, 5869−5878.
(19) Tsukamoto, K.; Tachibana, K.; Yamazaki, N.; Ishii, Y.; Ujiie, K.; Nishida, N.; Sawai, T. *Eur. J. Biochem.* **1990**, *188*, 15−22.
(20) Tsukamoto, K.; Nishida, N.; Tsuruoka, M.; Sawai, T. *FEBS Lett.* **1990**, *271*, 243−246.
(21) Monnaie, D.; Dubus, A.; Cooke, D.; Marchand-Brynaert, J.; Normark, S.; Frère, J.-M. *Biochemistry* **1994**, *33*, 5193−201.
(22) Dubus, A.; Normark, S.; Kania, M.; Page, M. G. P. *Biochemistry* **1994**, *33*, 8577−8586.
(23) Dubus, A.; Ledent, P.; Lamotte-Brasseur, J.; Frère, J.-M. *Proteins: Struct., Funct., Genet.* **1996**, *25*, 473−485.
(24) Oefner, C.; D'Arcy, A.; Daly, J. J.; Gubernator, K.; Charnas, R. L.; Heinze, I.; Hubschwerlen, C.; Winkler, F. K. *Nature* **1990**, *343*, 284−288.
(25) Beadle, B. M.; Trehan, I.; Focia, P. J.; Shoichet, B. K. *Structure* **2002**, *10*, 413−424.
(26) Díaz, N.; Suárez, D.; Sordo, T. L. *Biochemistry* **2006**, *45*, 439−451.
(27) Gherman, B. F.; Goldberg, S. D.; Cornish, V. W.; Friesner, R. A. *J. Am. Chem. Soc.* **2004**, *126*, 7652−7664.
(28) Tripathi, R.; Nair, N. N. *J. Phys. Chem. B* **2012**, *116*, 4741−4753.
(29) Page, M. I.; Vilanova, B.; Layland, N. J. *J. Am. Chem. Soc.* **1995**, *117*, 12092−12095.
(30) Chen, Y.; McReynolds, A.; Shoichet, B. K. *Protein Sci.* **2009**, *18*, 662−669.
(31) Lammote-Brasseur, J.; Dubus, A.; Wade, R. C. *Proteins: Struct., Funct., Genet.* **2000**, *40*, 23−28.
(32) Lobkovsky, E.; Billings, E. M.; Moews, P. C.; Rahil, J.; Pratt, R. F.; Knox, J. R. *Biochemistry* **1994**, *33*, 6762−6772.
(33) Wouters, J.; Fonze, E.; Vermeire, M.; Frere, J. M.; Charlier, P. *Cell. Mol. Life Sci.* **2003**, *60*, 1764−1773.
(34) Patera, A.; Blaszczak, L. C.; Shoichet, B. K. *J. Am. Chem. Soc.* **2000**, *122*, 10504−10512.
(35) Kato-Toma, Y.; Iwashita, T.; Masuda, K.; Oyama, Y.; Ishiguru, M. *Biochem. J.* **2003**, *371*, 175−181.
(36) Chen, Y.; Minasov, G.; Roth, T. A.; Prati, F.; Shoichet, B. K. *J. Am. Chem. Soc.* **2006**, *128*, 2970−2976.
(37) Sharma, S.; Bandyopadhyay, P. *J. Mol. Model.* **2012**, *18*, 481−492.
(38) Hata, M.; Tanaka, Y.; Fujii, Y.; Neya, S.; Hoshino, T. *J. Phys. Chem. B* **2005**, *109*, 16153−16160.
(39) Galleni, M.; Amicosante, G.; Frére, J.-M. *Biochem. J.* **1988**, *255*, 123−129.
(40) Warshel, A. *Computer Modeling of Chemical Reactions in Enzymes and Solutions*; John Wiley & Sons: New York, 1991.
(41) van der Kamp, M. W.; Mulholland, A. J. *Biochemistry* **2013**, *52*, 2708−2728.

(42) Warshel, A.; Levitt, M. *J. Mol. Biol.* **1976**, *103*, 227−249.
(43) Laio, A.; Parrinello, M. *Proc. Natl. Acad. Sci. U.S.A.* **2002**, *99*, 12562−12566.
(44) Iannuzzi, M.; Laio, A.; Parrinello, M. *Phys. Rev. Lett.* **2003**, *90*, 238302−1−4.
(45) Cheatham, T. E.; Cieplak, P.; Kollman, P. A. *J. Biomol. Struct. Dyn.* **1999**, *16*, 845−62.
(46) Wang, J.; Wolf, R. M.; Caldwell, J. W.; Kollman, P. A.; Case, D. A. *J. Comput. Chem.* **2004**, *25*, 1157−1173.
(47) RED: RESP ESP Charge Derive, version III.3; see http://q4md-forcefieldtools.org/RED/.
(48) Laio, A.; VandeVondele, J.; Rothlisberger, U. *J. Chem. Phys.* **2002**, *116*, 6941−6947.
(49) CPMD Program Package, version 13.2; IBM Corp., 1990−2011; MPI für Festkörperforschung Stuttgart, 1997−2001; see http://www.cpmd.org.
(50) Perdew, J. P.; Chevary, J. A.; Vosko, S. H.; Jackson, K. A.; Pederson, M. R.; Singh, D. J.; Fiolhais, C. *Phys. Rev. B* **1992**, *46*, 6671−6687.
(51) Vanderbilt, D. *Phys. Rev. B* **1990**, *41*, 7892−7895.
(52) Laio, A.; VandeVondele, J.; Rothlisberger, U. *J. Phys. Chem. B* **2002**, *106*, 7300−7307.
(53) Martyna, G. J.; Klein, M. L.; Tuckerman, M. *J. Chem. Phys.* **1992**, *97*, 2635−2643.
(54) Car, R.; Parrinello, M. *Phys. Rev. Lett.* **1985**, *55*, 2471−2474.
(55) Barducci, A.; Bonomi, M.; Parrinello, M. *WIREs Comput. Mol. Sci.* **2011**, *1*, 826−843.
(56) Ensing, B.; Laio, A.; Parrinello, M.; Klein, M. L. *J. Phys. Chem. B* **2005**, *109*, 6676−6687.
(57) Bussi, G.; Gervasio, F. L.; Laio, A.; Parrinello, M. *J. Am. Chem. Soc.* **2006**, *128*, 13435−13441.
(58) Piana, S.; Laio, A. *J. Phys. Chem. B* **2007**, *111*, 4553−4559.
(59) Dellago, C.; Bolhuis, P. G.; Csajka, F. S.; Chandler, D. *J. Chem. Phys.* **1998**, *108*, 1964−1977.
(60) Nair, N. N.; Schreiner, E.; Marx, D. *J. Am. Chem. Soc.* **2006**, *128*, 13815−13826.
(61) Zhao, Y.; Truhlar, D. G. *Theor. Chem. Acc.* **2008**, *120*, 215−41.
(62) Laio, A.; Rodriguez-Fortea, A.; Gervasio, F. L.; Ceccarelli, M.; Parrinello, M. *J. Phys. Chem. B* **2005**, *109*, 6714−6721.
(63) In this work, we defined a hydrogen bond in terms of the following geometric conditions: distances d[X−Y] < 3.4 Å and d[X−H] < 2.8 Å and angle θ[H−X···Y] < 30°, where X and Y can be either N or O.
(64) Kuzin, A. P.; Liu, H.; Kelly, J. A.; Knox, J. R. *Biochemistry* **1995**, *34*, 9532−9540.
(65) Lobkovsky, E.; Moews, P. C.; Liu, H.; Zhao, H.; Frère, J.-M.; Knox, J. R. *Proc. Natl. Acad. Sci. U.S.A.* **1993**, *90*, 11257−11261.
(66) Plantan, I.; Selic, L.; Mesar, T.; Anderluh, P. S.; Oblak, M.; Prezelj, A.; Hesse, L.; Andrejasic, M.; Vilar, M.; Turk, D.; Kocijan, A.; Prevec, T.; Vilfan, G.; Kocjan, D.; Copar, A.; Urleb, U.; Solmajer, T. *J. Med. Chem.* **2007**, *50*, 4113−4121.
(67) Meroueh, S. O.; Minasov, G.; Lee, W.; Shoichet, B. K.; Mobashery, S. *J. Am. Chem. Soc.* **2003**, *125*, 9612−9618.
(68) Trehan, I.; Beadle, B. M.; Shoichet, B. K. *Biochemistry* **2001**, *40*, 7992−7999.
(69) Fenollar-Ferrer, C.; Frau, J.; Donoso, J.; Muñoz, F. *Proteins: Struct., Funct., Genet.* **2003**, *51*, 442−452.
(70) Ehmann, D. E.; Jahič, H.; Ross, P. L.; Gu, R.-F.; Hu, J.; Kern, G.; Walkup, G. K.; Fisher, S. L. *Proc. Natl. Acad. Sci. U.S.A.* **2012**, *109*, 11663−11668.